
Distribution-Conditioned Transport: Zero-Shot Transport from Any Distribution to Any Distribution

000
001
002
003
004
005
006
007
008
009
010
011
012
013
014
015
016
017
018
019
020
021
022
023
024
025
026
027
028
029
030
031
032
033
034
035
036
037
038
039
040
041
042
043
044
045
046
047
048
049
050
051
052
053
054

Anonymous Authors¹

Abstract

1. Introduction

Learning transport maps between probability distributions is a central challenge across machine learning and the sciences. A wide variety of approaches, including diffusion and flow-based models, have addressed with great success the one-to-one transport problem: learning a map which pushes a source density P_0 to a target density P_1 (Goodfellow et al., 2014; Rezende & Mohamed, 2015; Genevay et al., 2018b; Liu et al., 2022; Lipman et al., 2023; Albergo et al., 2023b). However, a new class of problems is emerging where the goal is not only to model the evolution between a single pair of distributions, but rather to model dynamics in a way that can generalize across a broad range of source and target distributions.

A concrete motivating example of this shift can be seen in the study of cellular dynamics. Experimental techniques such as clonal lineage tracing have enabled the generation of datasets containing snapshots not just of a single cell population, but of thousands of distinct populations (clones) evolving in parallel (Biddy et al., 2018; Weinreb et al., 2020; Wagner & Klein, 2020). These datasets are sparse, in the sense that we do not observe the all time-marginals for all populations. For example, we may observe one population at both an initial time t_0 and a final time t_1 , while others are observed only at either t_0 or t_1 .

Two lines of literature have begun to approach this problem. Multimarginal stochastic interpolants offer an approach to learn dynamics between any pair of a fixed set of k distributions, solving a k -to- k transport problem (Albergo et al., 2023a), but cannot condition on a continuous space of distributions nor generalize to distributions unseen during training. In another direction, (Fishman et al., 2025) develop

approaches to learn “autoencoders” on the space of distributions by simultaneously learning to embed distributions and sample from the distribution conditional on that embedding. Meta flow matching (Atanackovic et al., 2024) is an early approach that leverages a heuristic distribution encoder for a structured transport problem. It embeds the source distribution with a distribution encoder coupled with a flow matching transport map. While effective in settings where many source-target pairs are available, if we observed many pairs of clonal lineages at both t_0 and t_1 , the MFM framework cannot ingest unpaired marginal distributions (e.g., cell populations observed at a single timepoint).

In this work we unify these perspectives. We first generalize and formalize the approach in (Atanackovic et al., 2024), demonstrating how distribution encoders developed in (Fishman et al., 2025) can be coupled with a broad class of transport models for source-conditioned transport. This immediately enables us to handle any-to-any transport by conditioning on both source and target distribution embeddings. This formulation enables us to generalize across distributions, predicting transport maps between population pairs unseen during training, as well as allowing us to make use of unstructured, partial observations (such as orphan marginals). We demonstrate the effectiveness of our approach first using a set of synthetic benchmark datasets, then on real-world applications ranging from image style transfer to learning cell population dynamics from lineage traced scRNA-seq data.

2. Methods

In many modern biological assays, we do not observe isolated datapoints in a vacuum. Instead, we repeatedly observe sets of measurements drawn from coherent biological entities that change in structured ways. Examples include (i) clonal lineages assayed at multiple timepoints in lineage tracing, (ii) cells from the same donor before and after a perturbation, and (iii) matched tissue microenvironments profiled under two experimental conditions. In many of these cases we are interested in a certain kind of counterfactual: what would these cells look like if they were in that state? This counterfactual problem is most naturally posed as a distributional transport problem, where we take

¹Anonymous Institution, Anonymous City, Anonymous Region, Anonymous Country. Correspondence to: Anonymous Author <anon.email@domain.com>.

Preliminary work. Under review by the International Conference on Machine Learning (ICML). Do not distribute.

055 a set of cells in one state and move them to another. Recent
 056 years have seen the development of a large number of meth-
 057 ods for distributional transport (Goodfellow et al., 2020;
 058 Genevay et al., 2018a; Lipman et al., 2022). These methods
 059 fundamentally transport one distribution to another; this
 060 process can be augmented by conditioning to transport one
 061 initial distribution to many different target states (model-
 062 ing differentiation for example) or many initial states to a
 063 corresponding target (like modeling a first time step to a
 064 second time step across many cell types). But we do not
 065 always have high-quality representations of the distributions
 066 we want to transport between.

067 To motivate this setting we focus on lineage tracing, where
 068 we observe many sets of clones of the same cell across
 069 different timepoints. The goal is to predict cell fate: to take
 070 the initial distribution of a clone and push it forward in time.
 071 Here, all cells are usually of the same “type”, so there is no
 072 natural way to represent the clone other than by the set of
 073 cells that define the clone. This requires modeling transport
 074 on the space of distributions. In this section we will outline
 075 tools for modeling on the space of distributions.

076 Formally, for an entity i (e.g. a clone), we observe a set of
 077 samples

$$S_i = \{x_{ij}\}_{j=1}^{m_i}, \quad x_{ij} \in \mathcal{X},$$

078 modeled as i.i.d. draws $x_{ij} \stackrel{\text{iid}}{\sim} P_i$ from some unknown dis-
 079 tribution $P_i \in \mathcal{P}(\mathcal{X})$.

080 The first tool we will develop here is a distribution encoder,
 081 which enables principled training of representations of sets of
 082 points as vectors. Then we will show how these distribution
 083 encoders can be linked to downstream transport models.

084 2.1. Distribution encoders: representing an empirical 085 population as a point in latent space

086 From each distribution we observe a finite sample set $S_i =$
 087 $\{x_{ij}\}_{j=1}^{m_i}$. We follow Fishman et al. (2025), defining a
 088 *distribution encoder*

$$\mathcal{E} : S_i \mapsto z_i \in \mathbb{R}^d,$$

089 which produces a fixed-dimensional embedding z_i intended
 090 to summarize the entire distribution P_i , rather than any
 091 particular cell. The key aim of distribution encoders is that
 092 z_i reflects only the underlying distributional signal and not
 093 sampling noise in S_i . To enforce this the encoder must be
 094 *distributionally invariant*. This imposes two invariances:

095 **Permutation invariance.** Reordering the samples in S_i
 096 does not change $\mathcal{E}(S_i)$.

097 **Proportional invariance.** Uniformly duplicating all sam-
 098 ples in S_i does not change $\mathcal{E}(S_i)$.

099 When these hold, the encoder can only depend on the em-
 100 pirical measure

$$\widehat{P}_i = \frac{1}{m_i} \sum_{j=1}^{m_i} \delta_{x_{ij}}.$$

101 In particular, there exists a measurable functional ϕ such
 102 that

$$\mathcal{E}(S_i) = \phi\left(\widehat{P}_i\right). \quad (1)$$

103 We refer to $z_i = \phi(\widehat{P}_{i,m})$ as a *distribution embedding*. A
 104 key property of such encoders is that they admit a central
 105 limit theorem (CLT). Let

$$z_i^* = \lim_{m_i \rightarrow \infty} \phi\left(\widehat{P}_i\right) = \phi(P_i)$$

106 denote the population-level embedding obtained in the
 107 infinite-sample limit. Under the invariances above and
 108 Hadamard differentiability of the pooling operator defin-
 109 ing ϕ , we have

$$\sqrt{m_i} (\mathcal{E}(S_i) - z_i^*) \xrightarrow{d} \mathcal{N}(0, \Sigma_i) \quad (2)$$

110 for a covariance Σ_i depending on P_i and the encoder \mathcal{E} .

111 For our purposes this CLT is the most important feature
 112 of distribution encoders because, as proved in (Fishman
 113 et al., 2025), it means that for any downstream loss we are
 114 interested in we can train models on moderate-sized sets
 115 at training time and compute gradients (in expectation) as
 116 though we were training using the true population embed-
 117 dings z_i^* .

118 2.2. Supervised (one-to-one) transport: 119 source-conditioning

120 A key setting for distributional transport is when we observe
 121 “pairs” of datasets. In our lineage tracing example this cor-
 122 responds to observing many clones across two timepoints,
 123 where we want to learn to transport from timepoint one to
 124 timepoint two. Another core example is when we observe
 125 many cell types under the same perturbation condition, our
 126 goal is to transport the unperturbed cells into their perturbed
 127 condition. This transport setting is analogous to supervised
 128 learning: we observe many source sets of cells and their
 129 corresponding target distribution and we want to learn a one-
 130 to-one map from the source to the target. In these settings
 131 it turns out by conditioning the the source distribution we
 132 can learn well defined transport maps. We will call these
 133 source-conditioned transport models.

134 A number of recent works have developed particular source-
 135 conditioned models such as (Atanackovic et al., 2024; Klein
 136 et al., 2025) in the context of flow matching or (He et al.,
 137 2025) using a direct MMD objective. Our notion of “source-
 138 conditioned” models generalizes these architectures under

a common framework and clarifies the underlying assumptions under which they enable distributional transport.

Formally, we will assume throughout this section that we have a supervised set of paired distributions sampled from some meta distribution (e.g. the set of clones sampled from the distribution of clones in the initial cell type)

$$(P_{1_{\text{src}}}, P_{1_{\text{tgt}}}), \dots (P_{n_{\text{src}}}, P_{n_{\text{tgt}}}) \sim Q,$$

and we observe empirical sets

$$S_{i_{\text{src}}} = \{x_{i_{\text{src}}, j}\}_{j=1}^{m_{i_{\text{src}}}} \sim P_{i_{\text{src}}} \text{ and } S_{i_{\text{tgt}}} = \{x_{i_{\text{tgt}}, j}\}_{j=1}^{m_{i_{\text{tgt}}}} \sim P_{i_{\text{tgt}}}.$$

We encode the *source* only so $z_{i_{\text{src}}} = \mathcal{E}(S_{i_{\text{src}}})$, where \mathcal{E} is a distribution encoder as laid out in Sec. 2.1. We can then learn a source-conditioned transport map acting on individual samples,

$$\mathcal{T}: \mathcal{X} \times \mathbb{R}^d \rightarrow \mathcal{X}, \quad x_{i_{\text{src}}} \mapsto \hat{x}_{i_{\text{tgt}}} = \mathcal{T}(x_{i_{\text{src}}} | z_{\text{src}}),$$

so that transported samples asymptotically follow the target distribution:

$$\mathcal{T}(S_{i_{\text{src}}} | \mathcal{E}(S_{i_{\text{src}}})) \xrightarrow[m_{i_{\text{src}}} \rightarrow \infty]{d} P_{i_{\text{tgt}}} \quad (3)$$

Here \mathcal{T} can be any conditional distributional transport model, and under a supervised pairing policy, the correct destination $P_{i_{\text{tgt}}}$ is implied once the source is specified.

We jointly fit \mathcal{E} and \mathcal{T} using the native loss of the chosen transport mechanism, written abstractly as

$$\mathcal{L}_{sc} = \ell(S_{\text{tgt}}, \mathcal{T}(S_{i_{\text{src}}} | \mathcal{E}(S_{i_{\text{src}}}))), \quad (4)$$

where ℓ may be a flow-matching objective (Atanackovic et al., 2024), a distributional divergence (e.g. Sinkhorn/MMD) (He et al., 2025), or any other generative transport model (see Sec 3.3). Because z_{src} obeys the CLT, we train with minibatches from S_{src} and S_{tgt} without biasing the population-level objective. After training, $\mathcal{T}(\cdot | \mathcal{E}(\cdot))$ can be applied to unseen sources to generate counterfactual realizations under their implied targets.

2.3. Unsupervised (any-to-any) transport: source-target conditioning

In many biological settings we do not have clean source-target pairings. Returning to our running lineage tracing case we actually only observe the same clone in both time-points a small fraction of the time. If we restrict ourselves to supervised transport models we have to throw away 90% of the clones we observe.

To leverage this additional data we develop an “unsupervised” analogue to the “supervised” transport setting. In the unsupervised world we simply have a set of unstructured distributions: $P_1, \dots, P_n \sim Q$ and associated samples:

$$S_i = \{x_{ij}\}_{j=1}^{m_i} \sim P_i$$

Our goal is to develop a model capable of learning to transport between any two distributions i and i' . Multimarginal stochastic interpolants (Albergo et al., 2023a) developed a class of models that can flow between any pair of distributions from a fixed initial set of K distributions by effectively embedding each distribution as a corner of the K -simplex and conditioning on the source and target corners. Our notion of source-target conditioned transport models leverage distribution encoders to learn distribution embeddings, enabling us to generalize to a new $(K + 1)^{\text{th}}$ distribution, and to embed a continuous number of distributions.

$$\mathcal{T}: \mathcal{X} \times \mathbb{R}^d \times \mathbb{R}^d \rightarrow \mathcal{X}, \quad x_i \mapsto \hat{x}_{i \rightarrow i'} = \mathcal{T}(x_i | z_i, z_{i'}),$$

to satisfy

$$\mathcal{T}(S_i | \mathcal{E}(S_i), \mathcal{E}(S_{i'})) \xrightarrow[m_i, m_{i'} \rightarrow \infty]{d} P_{i'} \quad (5)$$

Then using the same logic of the CLT we can train on samples using the objective conditioning on the encoder for the transport map of choice

$$\mathcal{L}_{\text{stc}} = \ell(S_{i'}, \mathcal{T}(S_i | \mathcal{E}(S_i), \mathcal{E}(S_{i'}))) \quad (6)$$

2.4. Semi-supervised transport: specializing source-target transport for supervised tasks

The goal for these unsupervised transport maps is really partial supervision: we want to train a transport map that can use all our data to learn a high-quality generative model, but at the end of the day we still care about prediction in the “paired” setting. There are two major points that are relevant for adapting source-target conditioned models to supervised tasks. First we outline how we can make latent predictions to enable supervised prediction from an unsupervised model; second we will comment on how we can choose pairings between source and target to leverage existing structure in the underlying distributions that “align” with the supervised task we are interested in.

To make this concrete, we can return to the lineage tracing case where we want to leverage all the clones, but the goal really is cell fate prediction. To actually convert the any-to-any model into a “supervised” model we can train a lightweight model to predict $z_{\text{src}} \mapsto z_{\text{tgt}}$ using the subset of paired (src, tgt) examples available for the task of interest; we then evaluate $\mathcal{T}(\cdot | z_{\text{src}}, \hat{z}_{\text{tgt}})$ to generate counterfactual samples “as if” drawn from P_{tgt} in a semi-supervised manner. For additional performance, we can actually co-train the “supervised” latent predictor along with the transport model by adding a predictor loss term

$$\mathcal{L}_{\text{cotrain}} = \mathcal{L}_{\text{stc}} + \lambda \cdot \ell'(z_{\text{tgt}}, \hat{z}_{\text{tgt}}), \quad (7)$$

with λ a weighing hyperparameter. This additional loss term regularizes the latent space learned by the encoder for downstream training of the lightweight model.

A second important practical point here is that we may not actually need nor want to learn to transport between any two distributions. Once more using the lineage tracing case for inspiration, it may make more sense to learn to transport any clone from timepoint one to any clone at timepoint two, instead of also learning allowing within timepoint and reverse time transport. The source-target conditioned model supports any-to-any inference but that does not mean we have to actually train on all pairs of datasets. We can instead choose a meta-distribution Q that defines a distribution over source-target pairs which we will train on. This allows analysts to encode relevant domain-specific structure into the underlying model through the design of Q . For example we can encourage the model to learn transport forward in time rather than the less structured any-to-any setting.

3. Related work

3.1. Distribution Embedding

Several lines of literature have tried to learn distribution embeddings or summary statistics. Kernel methods, such as kernel mean embedding (KME) and set kernels, provide nonparametric approaches to represent probability measures as points in a reproducing kernel Hilbert space, enabling tasks like distributional regression and classification (Smola et al., 2007; Muandet et al., 2012; Oliva et al., 2013; Szabo et al., 2015; Muandet et al., 2017). Our distribution embedding framework follows the formal framework in (Fishman et al., 2025) to learn distribution invariant-embeddings leveraging permutation-invariant architectures with a particular class of pooling operators (Zaheer et al., 2017; Wagstaff et al., 2021; Zhang et al., 2022).

3.2. Distribution Transport

Meta Flow Matching (Atanackovic et al., 2024) develops the idea of source-conditioning for learning transport maps across contexts. Our notion of source-conditioned models generalizes their approach to a broader class of transport models and demonstrates the conditions under which we can expect it to achieve (3). In single cell RNA-seq modeling there are a number of recent works that are effectively source-conditioned models (Klein et al., 2025; He et al., 2025; Adduri et al., 2025) as it is a useful technique for generalizing across cell types.

Multimarginal stochastic interpolants (MMSI) are the closest analogue to our any-to-any transport, except they require

a fixed set of K distributions (Albergo et al., 2023a) and enforce transport paths that go through “all” distributions to learn a barycenter, while we adaptively learn our transport paths through the distribution space. MMSI models “time” on the simplex, where each point in the simplex corresponds to an interpolant taking a convex combination of a sample from each of the K distributions proportional to their simplicial weight. The key choice here is what paths through the simplex to choose. If we consider the “edge path” where we flow directly between two corners of the simplex with no weight on other distributions then MMSI is a stochastic interpolant (or equivalently flow matching) transport model paired with a one-hot distribution encoder, but instead of flexibly combining $z_i, z_{i'}$ and t the model operates on $tz_i + (1-t)z_{i'}$, forcing the model to combine its understanding of time and the distribution embedding.

Style-transfer and unpaired image-translation methods provide a complementary line of work. Classical neural style transfer (Gatys et al., 2015; 2016) encodes “style” implicitly via Gram matrices of CNN features, but does not define an explicit or generalizable latent representation of the style domain. Multi-domain translation frameworks such as CycleGAN, StarGAN, and MUNIT (Zhu et al., 2017; Choi et al., 2018; Huang et al., 2018) condition the generator on a domain identifier, typically a one-hot categorical label or an instance-level style code. These approaches are restricted to a fixed, finite set of domains and cannot generalize transport to a new domain without retraining. In contrast, our source–target–conditioned transport learns *distribution embeddings* directly from sets of samples, enabling conditioning on a continuous family of contexts and permitting transport to previously unseen distributions.

3.3. Transport Models

A wide range of generative transport mechanisms can be used as the conditional map $\mathcal{T}(\cdot | z)$ or $\mathcal{T}(\cdot | z, z')$ in our framework. Classical adversarial approaches learn source–target mappings via discriminators, including GANs (Goodfellow et al., 2014) and Wasserstein GANs (Arjovsky et al., 2017). Kernel-based methods transport distributions by matching maximum mean discrepancy (MMD), as in generative moment matching networks (Li et al., 2015). Optimal-transport–based generative models construct maps using entropic or Sinkhorn divergences (Genevay et al., 2018b). Normalizing flows provide invertible transport parameterizations through continuous change-of-variable models (Rezende & Mohamed, 2015). Continuous-time flow-based models, such as flow matching, rectified flows, and stochastic interpolants (Lipman et al., 2023; Liu et al., 2022; Albergo et al., 2023b), define transport by learning a velocity field along a path interpolating between source and target.

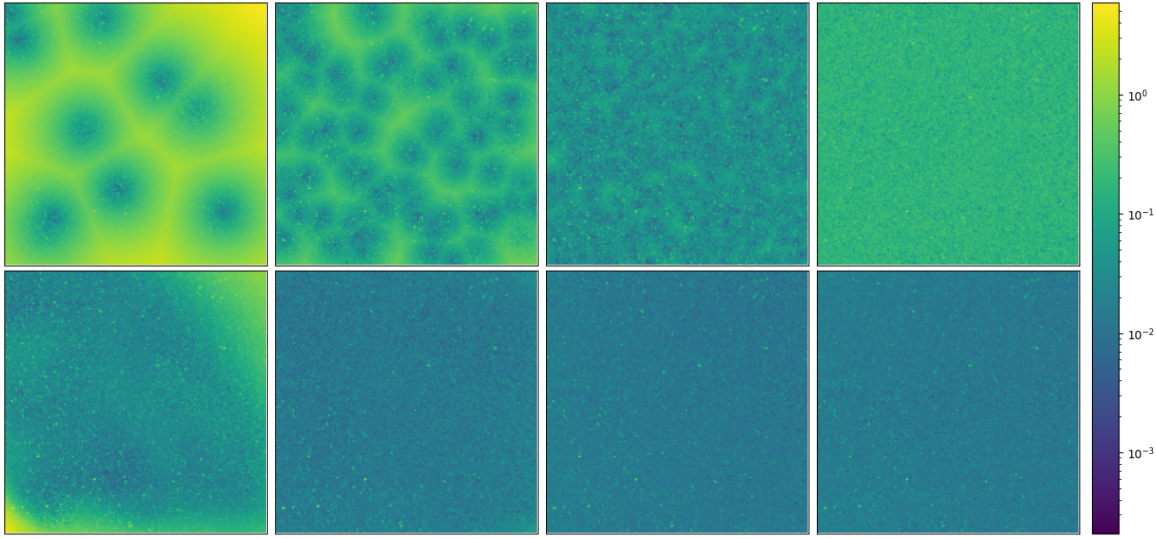


Figure 1. We compare a K -to- K transport model to the source-target conditioned any-to-any model for learning to transport between Gaussian distributions. We plot the W_2 distance between true and transported datapoints for all values of $\mu \in [0, 5]^2$. The top row in the K -to- K model, the bottom is the any-to-any model. Each column corresponds to models trained on different numbers of distributions $K = 10, 100, 1,000, 10,000$, but we fix the number of sample sets at $n = 50,000$. For the K -to- K model we compute the closest dataset in its set of K and use that as the prediction, which gives rise to the Voronoi-like structure in the first several plots; for the any-to-any model we can simply embed the target. For all K the any-to-any model achieves much better and more uniform transport. For $K = 10,000$ we also see the complete breakdown of the K -to- K model as it fails to learn high-quality embeddings for every distribution.

On discrete sequences, unsupervised machine translation methods (Lample et al., 2018a; Artetxe et al., 2018; Lample et al., 2018b) learn bidirectional maps between languages using only monolingual corpora, providing a discrete analogue of our unpaired any-to-any transport between distributions. More recently, flow-matching ideas have been extended to discrete domains via discrete flow matching and related categorical flow-matching frameworks that operate directly on probability simplices (Gat & Lipman, 2024; Cheng et al., 2024; Davis et al., 2024).

All of these models define mappings that take samples from a source distribution and produce samples matching a target distribution. Our framework is orthogonal to the specific transport mechanism: any such model can be conditioned on distribution embeddings to yield a source-conditioned or source–target–conditioned transport map that satisfies the population-level limits in (3) and (5).

4. Unsupervised Learning Enables Zero-Shot Transport

4.1. Gaussian Transport

As a first illustration, we study transport between simple Gaussian distributions, where we can control the data-generating process and directly visualize performance. This experiment introduces the main com-

ponents of our framework—distribution encoders and source–target–conditioned transport maps—in a setting where the ground-truth structure is transparent.

We construct a dataset of bivariate normal distributions by sampling parameters (μ_i, Σ_i) , $i = 1, \dots, n$, with means $\mu_i \in [0, 5]^2$ drawn from a uniform prior and covariances $\Sigma_i \in \mathbb{R}^{2 \times 2}$ drawn from a simple inverse-Wishart prior (see App. ?? for details). We then choose $K \in \{10, 100, 1,000, 10,000\}$ distinct parameter sets and draw $n = 50,000$ sample sets so that each distribution contributes n/K sample sets to the dataset.

For each value of K we train two models on the same dataset. The first is a conventional K -to- K architecture that treats each of the K distinct Gaussians as a discrete label (a “corner”) and learns transport conditional on the distribution-specific labels. At test time this model has no way to condition on a new target distribution, so we follow the natural baseline of assigning each target to its nearest training distribution and using that as the target condition. The second is our *source–target conditioned* model from Sec. 2.3, which encodes both source and target sets via the distribution encoder $z_i = \mathcal{E}(S_i)$ and learns a transport map $\mathcal{T}(x | z_{\text{src}}, z_{\text{tgt}})$ that can operate between arbitrary pairs of distributions, including unseen targets. For these experiments we use a mean-pooled DeepSets encoder as \mathcal{E} and a flow matching model as the transport map. The flow matching architectures are identical across models, with

<i>K</i>	<i>K-to-K</i> W_2^2	<i>Any-to-any</i> W_2^2
10	0.7779	0.0870
100	0.1369	0.0166
1,000	0.0435	0.0150
10,000	0.1683	0.0157

Table 1. Quantitative averages of the results visualized in Fig. 1. The any-to-any model performs substantially better overall and, unlike the *K-to-K* baseline, does not degrade when the number of distinct distributions *K* becomes very large.

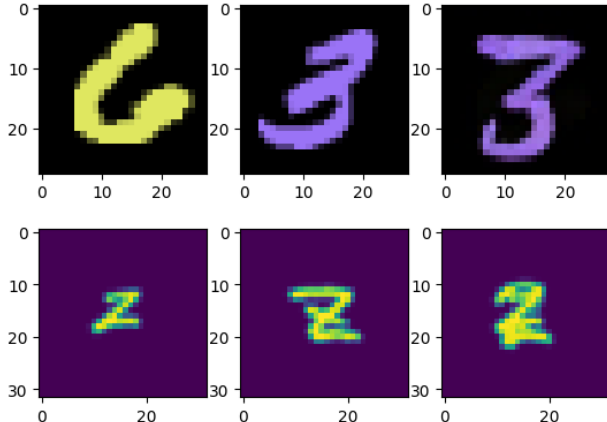


Figure 2. Here we present two examples of image style transfer. The first image is the sample from the source distribution, the second is a sample from the target distribution, and the third image is the first image transported to the target distribution conditioning on the source and target embeddings. Both tasks use completely heldout source and target distributions illustrating the model’s capacity for zero-shot generalization.

embeddings of the same dimension.

To visualize zero-shot performance we fix a single source distribution from the training set and evaluate transport to a dense grid of target parameters $\mu \in [0, 5]^2$ with corresponding random covariances Σ . The results are visualized in Fig. 1, and a quantitative comparison is given in Table 1.

4.2. Unsupervised Style Transfer

We can also leverage our any-to-any transport model for style transfer on images without language embeddings when the data are grouped into coherent distributions. Our goal here is not to propose a competitive method for classical image style transfer, where styles are typically specified by language tags and each tag may correspond to only a handful of images. In such settings, high-quality language embeddings already provide a natural representation of “style,” so there is little need to learn separate distribution encoders. Instead, this experiment serves as a sanity check demon-

strating that, when images are partitioned into clean sets, our approach can learn transport maps between these image distributions—a situation that more closely mirrors our biological applications, where we often lack high-quality side information to condition on.

MNIST Colors We first use the MNIST dataset to illustrate style transfer in this distributional setting. Each distribution is defined by a particular RGB color and digit class, e.g., “yellow sixes” or “purple threes.” By training on a large number of colors we can teach the model to zero-shot transport between digit-color distributions. We illustrate this in Fig. 2 where we use heldout colors to demonstrate how the model can map from yellow sixes to purple threes.

EMNIST Handwriting We next consider the EMNIST dataset, where we treat each writer as a “style” and each character as content. We form one distribution per (writer, character) pair by collecting all images of that character written by a given writer, and train the any-to-any model to transport between these distributions. At test time we evaluate zero-shot style transfer between unseen writers: the model is given source and target sets from writers that were never observed during training and must map individual characters from the source style to the target style. In Fig. 2 we show a representative example for two heldout authors and the letter “z,” where our model successfully transfers from a writer who draws a simple diagonal “z” with no crossbar to a writer whose “z” has a horizontal crossbar.

5. Improving Semi-supervised Learning

In the following we present a wide range of applications of TDEs that demonstrate how our method can be applied to multiple very different domains and perform well across the board.

5.1. Forecasting

Forecasting time-series data is a natural application of distribution transport models. Recent work () introduced two forecasting benchmarks for point clouds in ocean current trajectories and PBMC development trajectories (see Appendix ... for details).

In a supervised approach such as MFM a model is trained to transport only from one time point to the next. When training TDEs in this manner, so by pairing adjacent time points only, we achieve performance that while not terrible is not able to beat the SoTA.

We therefore trained our model in a semi-supervised manner in which we pair between any two time points during training. In a first attempt we first train the encoder and generator in a fully unsupervised manner and subsequently

Table 2. Gulf of Mexico Vortex Forecast

Method	GoM	PBMC
snapMMD	0.66(0.031)	0.0042(0.0017)
SBIRR-ref	0.35(0.032)	0.097(0.060)
SBIRR-forward	0.62(0.054)	0.51(0.16)
MFM	0.249(0.105)	0.014(0.006)
TDEs		
any-to-any	0.61(0.112)	0.0062(0.0035)
any-to-any, cotrained	0.15(0.113)	0.0039(0.0019)
any-to-any, unlabeled	0.34(0.078)	0.0046(0.0031)

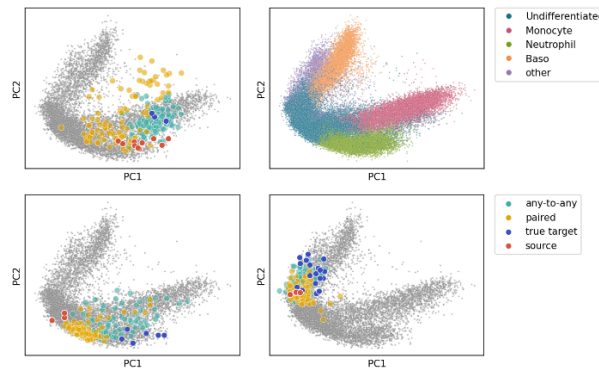


Figure 3. Any-to-any vs. paired pushforward prediction on ([Weinreb et al., 2020](#)). Visualizing first 2 PCs of true and generated data. Each subplot shows a single clone, chosen based on difference between energy distance of predictions between models.

Method	Energy Distance ↓
Paired (supervised)	3.43 ± 0.10
Any-to-any (semi-supervised)	3.17 ± 0.09

Table 3. Comparison of pushforward performance on the [Weinreb et al. \(2020\)](#). We report the mean \pm s.e.m of energy distance (lower is better) across 628 held-out test clones.

train a latent predictor in a supervised manner on frozen encoder embeddings. This approach of completely separating the unsupervised and supervised parts of training yields low performance comparable to the supervised approach. The reason is that there is no imperative for the encoder to nicely structure the latent space and since the encoder collapses distributions into a single vector in latent space, if a time-series dataset consists of only 10-20 time points the training dataset for the predictor model will be very small. We therefore co-train the ridge regressor with the encoder-generator pair, achieving SOTA performance on both benchmarks.

A further extension of the any-to-any pairing approach is to incorporate data that lacks a time label, so data that cannot be used for supervised training. Here, the larger amount of data that this gives us allows us to increase performance compared to the regular any-to-any pairing, although not quite as high MMD scores as the cotrained any-to-any approach. The explanation for this is that while this trains on more data, the lack of an explicit time label prohibits cotraining the latent predictor model during large parts of training, leading to a less structured latent space.

5.2. Clonal population dynamics

We next apply TDEs to learn clonal population dynamics using lineage-traced single-cell RNA-sequencing (scRNA-seq) data from [Weinreb et al. \(2020\)](#). A critical challenge in this dataset is sparsity: there are about $6 \cdot 10^3$ clones measured in total, however only about $2 \cdot 10^3$ of these clones are profiled at multiple timepoints. The majority of clones are “orphans” observed only at a single timepoint.

While source-conditioned approaches can only be trained on clones observed at multiple timepoints, training TDEs with any-to-any pairings allow us to make use of all available marginals. To assess the benefit of moving to the semi-supervised paradigm, we compare two training approaches. First is a baseline which is exclusively trained on paired clones, akin to meta-flow matching. Second is an any-to-any model trained on all pairs of observed marginals.

Both settings use an identical architecture operating on the first 50 principal components (PCs) of the gene expression profiles. The model consists of a mean-pooled deep sets encoder and an energy-based model generator. For latent prediction, we use a post-hoc ridge regression. As shown in Table 5.2, the any-to-any training objective outperforms the source-conditioned baseline, demonstrating the benefit of incorporating unpaired clones into the learning process. In Fig.3, we visualize the predictions of three clones which have large differences between the two models.

Impact Statement

This paper presents work whose goal is to advance the field of Machine Learning. There are many potential societal consequences of our work, none which we feel must be specifically highlighted here.

References

- Adduri, A. K., Gautam, D., Bevilacqua, B., Imran, A., Shah, R., Naghipourfar, M., Teyssier, N., Ilango, R., Nagaraj, S., Dong, M., et al. Predicting cellular responses to perturbation across diverse contexts with state. *bioRxiv*, pp. 2025–06, 2025.

Albergo, M. S., Boffi, N. M., Lindsey, M., and Vandenberghe, P. Deep generative models for joint cell type and clone identification. *bioRxiv*, pp. 2025–06, 2025.

- 385 Eijnden, E. Multimarginal generative modeling with
 386 stochastic interpolants. *arXiv preprint arXiv:2310.03695*,
 387 2023a.
- 388 Albergo, M. S., Boffi, N. M., and Vanden-Eijnden, E.
 389 Stochastic interpolants: A unifying framework for flows
 390 and diffusions. *Journal of Machine Learning Research*,
 391 24:1–63, 2023b.
- 392 Arjovsky, M., Chintala, S., and Bottou, L. Wasserstein
 393 GAN. In *Proceedings of the 34th International Conference*
 394 *on Machine Learning*, volume 70, pp. 214–223. PMLR,
 395 2017.
- 396 Artetxe, M., Labaka, G., Agirre, E., and Cho, K. Unsupervised
 397 neural machine translation. In *International Conference*
 398 *on Learning Representations*, 2018.
- 400 Atanackovic, L., Zhang, X., Amos, B., Blanchette, M., Lee,
 401 L. J., Bengio, Y., Tong, A., and Neklyudov, K. Meta Flow
 402 Matching: Integrating Vector Fields on the Wasserstein
 403 Manifold. In *The Thirteenth International Conference on*
 404 *Learning Representations*, 4 October 2024.
- 405 Biddy, B. A., Kong, W., Kamimoto, K., Guo, C., Waye,
 406 S. E., Sun, T., and Morris, S. A. Single-cell mapping
 407 of lineage and identity in direct reprogramming. *Nature*,
 408 564(7735):219–224, 2018.
- 409 Cheng, X., Chen, T., Li, K., Gao, R., Zhu, J., and Liu, Q.
 410 Categorical flow matching. In *International Conference*
 411 *on Learning Representations*, 2024.
- 412 Choi, Y., Choi, M., Kim, M., Ha, J.-W., Kim, S., and Choo,
 413 J. StarGAN: Unified generative adversarial networks for
 414 multi-domain image-to-image translation. In *Proceedings*
 415 *of the IEEE Conference on Computer Vision and Pattern*
 416 *Recognition (CVPR)*, pp. 8789–8797, 2018.
- 417 Davis, N., Chen, R. T. Q., Hu, Y., and Rezende, D. J. Fisher
 418 flow matching: Transport in the probability simplex. In
 419 *International Conference on Machine Learning*, 2024.
- 420 Fishman, N., Gowri, G., Yin, P., Gootenberg, J., and Abu-
 421 dayyeh, O. Generative distribution embeddings. *arXiv*
 422 *preprint arXiv:2505.18150*, 2025.
- 423 Gat, I. and Lipman, Y. Discrete flow matching. In *Advances*
 424 *in Neural Information Processing Systems*, 2024.
- 425 Gatys, L. A., Ecker, A. S., and Bethge, M. A neural algo-
 426 rithm of artistic style. *arXiv preprint arXiv:1508.06576*,
 427 2015.
- 428 Gatys, L. A., Ecker, A. S., and Bethge, M. Image style trans-
 429 fer using convolutional neural networks. In *Proceedings*
 430 *of the IEEE Conference on Computer Vision and Pattern*
 431 *Recognition (CVPR)*, pp. 2414–2423, 2016.
- 432 Genevay, A., Peyré, G., and Cuturi, M. Learning Generative
 433 Models with Sinkhorn Divergences. In *International Conference*
 434 *on Artificial Intelligence and Statistics*, pp. 1608–1617. PMLR, 31 March 2018a.
- 435 Genevay, A., Peyré, G., and Cuturi, M. Learning generative
 436 models with sinkhorn divergences. In *Proceedings of the Twenty-First International Conference on Artificial Intelligence and Statistics*, volume 84, pp. 1608–1617. PMLR, 2018b.
- 437 Goodfellow, I., Pouget-Abadie, J., Mirza, M., Xu, B.,
 438 Warde-Farley, D., Ozair, S., Courville, A., and Bengio,
 439 Y. Generative adversarial nets. In *Advances in Neural Information Processing Systems*, volume 27, 2014.
- 440 Goodfellow, I., Pouget-Abadie, J., Mirza, M., Xu, B.,
 441 Warde-Farley, D., Ozair, S., Courville, A., and Bengio,
 442 Y. Generative adversarial networks. *Communications of the ACM*, 63(11):139–144, 22 October 2020. ISSN
 0001-0782,1557-7317. doi: 10.1145/3422622.
- 443 He, C., Zhang, J., Dahleh, M., and Uhler, C. Morph predicts
 444 the single-cell outcome of genetic perturbations across
 445 conditions and data modalities. *bioRxiv*, 2025.
- 446 Huang, X., Liu, M.-Y., Belongie, S., and Kautz, J. Multi-
 447 modal unsupervised image-to-image translation. In *Proceedings*
 448 *of the European Conference on Computer Vision (ECCV)*, pp. 179–196, 2018.
- 449 Klein, D., Fleck, J. S., Bobrovskiy, D., Zimmermann, L.,
 450 Becker, S., Palma, A., Dony, L., Tejada-Lapuerta, A.,
 451 Huguet, G., Lin, H.-C., et al. Cellflow enables generative
 452 single-cell phenotype modeling with flow matching. *bioRxiv*, pp. 2025–04, 2025.
- 453 Lample, G., Conneau, A., Denoyer, L., and Ranzato, M.
 454 Unsupervised machine translation using monolingual cor-
 455 pora only. In *International Conference on Learning Rep-
 456 resentations*, 2018a.
- 457 Lample, G., Ott, M., Conneau, A., Denoyer, L., and Ran-
 458 zato, M. Phrase-based & neural unsupervised machine
 459 translation. In *Proceedings of the 2018 Conference on Empirical Methods in Natural Language Processing*, pp.
 460 5039–5049. Association for Computational Linguistics,
 461 2018b.
- 462 Li, Y., Swersky, K., and Zemel, R. S. Generative moment
 463 matching networks. In *Proceedings of the 32nd Interna-
 464 tional Conference on Machine Learning*, volume 37, pp.
 465 1718–1727. PMLR, 2015.
- 466 Lipman, Y., Chen, R. T. Q., Ben-Hamu, H., Nickel, M.,
 467 and Le, M. Flow Matching for generative modeling. *International Conference on Learning Representations*,
 468 abs/2210.02747, 6 October 2022.

- 440 Lipman, Y., Chen, R. T. Q., Ben-Hamu, H., Nickel, M.,
 441 and Le, M. Flow matching for generative modeling. In
 442 *International Conference on Learning Representations*,
 443 2023.
- 444
- 445 Liu, X., Gong, C., and Liu, Q. Flow straight and fast:
 446 Learning to generate and transfer data with rectified flow.
 447 In *Advances in Neural Information Processing Systems*,
 448 volume 35, 2022.
- 449
- 450 Muandet, K., Fukumizu, K., Dinuzzo, F., and Schölkopf,
 451 B. Learning from distributions via support measure
 452 machines. *Neural Information Processing Systems*, 25:10–
 453 18, 29 February 2012.
- 454
- 455 Muandet, K., Fukumizu, K., Sriperumbudur, B., and
 456 Schölkopf, B. Kernel mean embedding of distributions: A
 457 review and beyond. *Foundations and Trends® in Machine
 458 Learning*, 10(1-2):1–141, 2017. ISSN 1935-8237,1935-
 459 8245. doi: 10.1561/2200000060.
- 460
- 461 Oliva, J. B., Póczos, B., and Schneider, J. Distribution to
 462 Distribution Regression. *International Conference on
 463 Machine Learning*, 28(3):1049–1057, 16 June 2013.
- 464
- 465 Rezende, D. J. and Mohamed, S. Variational inference with
 466 normalizing flows. In *Proceedings of the 32nd Interna-*

467 *tional Conference on Machine Learning*, volume 37, pp.
 468 1530–1538. PMLR, 2015.

469

470 Smola, A., Gretton, A., Song, L., and Schölkopf, B. A
 471 Hilbert space embedding for distributions. In *Lecture
 472 Notes in Computer Science*, Lecture notes in computer sci-
 473 ence, pp. 13–31. Springer Berlin Heidelberg, Berlin, Hei-
 474 delberg, 2007. ISBN 9783540752240,9783540752257.
 475 doi: 10.1007/978-3-540-75225-7\5.

476

477 Szabo, Z., Gretton, A., Poczos, B., and Sriperumbudur, B.
 478 Two-stage sampled learning theory on distributions. In
 479 *Artificial Intelligence and Statistics*, pp. 948–957. PMLR,
 21 February 2015.

480

481 Wagner, D. E. and Klein, A. M. Lineage tracing meets
 482 single-cell omics: opportunities and challenges. *Nature
 483 Reviews Genetics*, 21(7):410–427, 2020.

484

485 Wagstaff, E., Fuchs, F., Engelcke, M., Osborne, M. A., and
 486 Posner, I. Universal approximation of functions on sets.
 487 *Journal of machine learning research: JMLR*, 23(151):
 488 151:1–151:56, 5 July 2021. ISSN 1532-4435,1533-7928.

489

490 Weinreb, C., Rodriguez-Fraticelli, A., Camargo, F. D., and
 491 Klein, A. M. Lineage tracing on transcriptional land-
 492 scapes links state to fate during differentiation. *Science*,
 493 367(6479), 14 February 2020. ISSN 0036-8075,1095-
 494 9203. doi: 10.1126/science.aaw3381.

Zaheer, M., Kottur, S., Ravanbakhsh, S., Póczos, B.,
 Salakhutdinov, R., and Smola, A. Deep Sets. *Advances
 in neural information processing systems*, 30, 10 March
 2017.

Zhang, L. H., Tozzo, V., Higgins, J., and Ranganath, R.
 Set norm and equivariant skip connections: Putting the
 deep in Deep Sets. *International Conference on Machine
 Learning*, 162:26559–26574, 23 June 2022. doi: 10.
 48550/arXiv.2206.11925.

Zhu, J.-Y., Park, T., Isola, P., and Efros, A. A. Unpaired
 image-to-image translation using cycle-consistent adver-
 sarial networks. In *Proceedings of the IEEE International
 Conference on Computer Vision (ICCV)*, pp. 2223–2232,
 2017.

495 **A. Gulf of Mexico**

496 **A.1. Dataset preprocessing details**

498 This dataset consists of the trajectories of 400 particles flowing along an ocean current. It was generated by integrating the
499 velocity field of a vortex observed in the Gulf of Mexico on June 1st, 2024 at 5pm. Initial positions were sampled within a
500 small radius and the positions across 11 time points make up the dataset. The final time point is held out for the forecasting
501 benchmark.

502 **A.2. TDE architecture and training details**

505 We train a mean-pooled fully connected MLP as the distribution encoder and an energy-based model (EBM) as the generator
506 (need to add details of EBM). Models were trained over 1,000 epochs with the ADAM optimizer and learning rate $\eta = \dots$.
507 We train the predictor model after the training of encoder and generator has completed in a supervised manner, training it to
508 map the latent representation between consecutive time points. Due to the compressed nature of our distribution embeddings,
509 we train a simple ridge regressor with $\alpha = \dots$. The dataset for the predictor is generated by encoding $N = \dots$ subsets
510 sampled at random for each time point. To better structure the latent space for the downstream training of the predictor
511 model, we cotrain a similar ridge regression model along the encoder and generator models and add a small loss term (cosine
512 distance) to the training loss.

513 **B. PBMC**

514 **B.1. Dataset preprocessing details**

517 This dataset consists of a 30-dimensional projection of single-cell RNA-sequencing data of peripheral blood mononuclear
518 cells (PBMCs) that were collected every hour for 21 hours. Here we hold out the last hour for forecasting validation.

520 **B.2. TDE architecture and training details**

521 TDE architecture follows the same structure as our implementation for the GoM task. Need to add hyperparameters used.

524 **C. GISAID spike protein sequences**

526 **C.1. Dataset preprocessing details**

528 This dataset consists of SARS-CoV2 spike protein sequences over time and location. We used data from the Global Initiative
529 on Sharing All Influenza Data (GISAID) up to and including January 2025. Sequences were grouped by sampling month
530 and location (country and state), and each group was treated as an empirical distribution of protein sequences. Entries with
531 invalid date fields and ambiguous or undetermined residues were removed. For tokenization, sequences were truncated to
532 1000 amino acids.

533 **C.2. TDE architecture and training details**

535 The encoder consists of multi-head self-attention blocks stacked on mean-pooled embeddings generated by the ESM2-8M
536 model. For the generator we finetune another instance of the ESM2-8M model with a discrete flow matching objective to
537 mutate source sequences into target sequences. Both for the encoder and the generator, we load the pretrained weights but
538 do not freeze them.

539 (Predictor still needs to be trained, will probably be similar to the other datasets, so just ridge regression of some sort).

541
542
543
544
545
546
547
548
549

550 **D. Hematopoiesis lineage-tracing scRNA-seq**551 **D.1. Dataset preprocessing details**552 **D.2. TDE architecture and training details**553 **E. Implementations of baseline methods**554 **E.1. Meta flow matching**

558 For the implementation of MFM we follow the details of the original paper (): the encoder architecture consists of a
559 mean-pooled GNN that receives a kNN graph with $k = \dots$ of the source samples as input. For the generator, we use a
560 flow-matching archiecture. In contrast to TDEs, we condition the generator only on the source latent embeddings, so with
561 no conditioning on the target latent.

562 **E.2. SnapMMD**

563 Just using the results from the paper (and when I fiddled around with it I just used the code they uploaded to github together
564 with their implementation).

565 **E.3. other baselines you may have tried**

566 None

567

568

569

570

571

572

573

574

575

576

577

578

579

580

581

582

583

584

585

586

587

588

589

590

591

592

593

594

595

596

597

598

599

600

601

602

603

604